Experimental Mechanics
DOI 10.1007/s11340-011-9521-0

In Situ Optical Investigations of Hypervelocity Impact Induced Dynamic Fracture

L. Lamberson · V. Eliasson · A.J. Rosakis

Received: 31 January 2011 / Accepted: 12 June 2011

Abstract One of the prominent threats in the endeavor to develop next-generation space assets is the risk of space debris impact in earth's orbit and micrometeoroid impact damage in deep space. To date, there is no study available which concentrates on the analysis of dynamic crack growth from hypervelocity impacts on such structures, resulting in their eventual catastrophic degradation. Experiments conducted using a unique two-stage light-gas gun facility have examined the *in situ* dynamic fracture of brittle polymers subjected to this high-energy-density event. Optical techniques of caustics and photoelasticity, combined with high-speed photography, analyze crack growth behavior of Mylar and Homalite 100 thin plates after impact at velocities ranging from 3 to 7 km/s (7,000–15,500 mph). Results indicate that even under extreme impact conditions of out-of-plane loading, highly localized heating, and energetic impact phenomena involving plasma formation and ejecta, the dynamic fracture process occurs during a deformation regime dominated by in-plane loading.

L. Lamberson · A.J. Rosakis (SEM fellow)
Graduate Aerospace Laboratories, California Institute of Technology, Pasadena, CA 91125, USA

V. Eliasson
Department of Aerospace & Mechanical Engineering, University of Southern California, Los Angeles, CA 90089, USA

Present Address:
L. Lamberson (✉, SEM member)
Johns Hopkins University, Baltimore, MD 21218, USA
e-mail: lamberson@jhu.edu

Keywords Hypervelocity · Dynamic fracture · Brittle polymer · Stress intensity · Energy release rate

Introduction

The International Space Station (ISS) includes over one-hundred different types of shielding and still executes debris avoidance procedures [1]. While large pieces of space debris are tracked by the United States Space Command, there are an estimated 50,000 pieces of un-cataloged space debris larger than 1 cm in diameter, with potentially trillions more untracked under 1 cm in diameter. Although relatively small in size, space debris collisions average 10 km/s and at this rate, a 1 cm diameter debris can, on impact, deliver double the kinetic energy of a 250 kg object traveling at 100 km/hr [2]. Consequently micrometeoroid and space debris traveling at hypervelocity have the ability to compromise or deplete not only the structural integrity of a space asset, but also the electrical, thermal, and optical functionality.

The hypervelocity regime is initiated at an impact speed so great, the inertial stresses outweigh the material strength. For materials considered in this study, it is speeds in excess of about 1–2 km/s (2,200–4,500 mph). In the context of examining the dynamic fracture behavior of brittle materials, we define hypervelocity as speeds on the order of, or greater than, the shear wave speed or c_s of the impacted solid. In our study, impact speeds are approximately two to three times the maximum speed at which the material can propagate information through its microstructure. As a result, damage and failure mechanisms discussed in existing impact literature on brittle materials examined at lower than

Published online: 23 July 2011

hypervelocity, and consequently lower kinetic energy densities, may not be valid. Therefore a critical need to experimentally examine material behavior at these extreme material conditions exists.

Metal response from hypervelocity impact, typically in the context of a Whipple bumper shield for micrometeroid and space debris impact, has been under extensive investigation by NASA since the birth of space exploration [3]. In this regard, thin metallic sheets are tested in the hypervelocity regime to evaluate a ballistic limit as a means to correlate the velocity of the impactor to a resulting damage length scale. Although metals are a large component of most space assets, more brittle materials such as polymers and ceramics in the form of thin tiles are often significant components of optical and thermal protection systems of space structures. Specifically, nominally brittle materials such as silica glass used in the 'window to the world' Cupola recently completed on the ISS [4], and Kapton, a Mylar-like polymer used on the tennis court-sized sunshield for the James Webb Space Telescope scheduled to launch in 2013 [5], are particularly vulnerable to dynamic crack propagation resulting from potential space debris or micrometeoroid impacts.

Experimental Background

A unique two-stage light-gas gun facility was used to experimentally investigate hypervelocity impacts. Originally designed by Southwest Research Institute and completed in 2006 [6], this particular gun is a joint venture between the California Institute of Technology and NASA's Jet Propulsion Laboratory (JPL), known as the Small Particle Hypervelocity Impact Range (SPHIR). Launch capability using slug impactor technology with masses between 5 to 50 mg of polymer or metal composition includes 0.9 grams of smokeless gun powder and rifle primers for detonation, and hydrogen gas to accelerate projectiles to impact velocities between 1 and 7 km/s. The facility itself is approximately 6 m in total length with a smooth-bore design, flight tube length of 3 m, and a large target chamber housing over a dozen optical ports (shown in Fig. 1).

In this study we were able to characterize the dynamic behavior *in situ* or during the impact and crack propagation, as well as determine the dominant failure mode. Thin target plates (1.6 mm) of two different brittle polymers, Mylar and Homalite 100, were used. Each plate was 150 mm in diameter with a center hole 20 mm in diameter that was initially pre-cracked. The plates were then subjected to far-field quasi-static tensile loads ranging from 0.5 to 4 MPa, similar in magnitude to a functional load on a component of a space asset, or possibly a hoop stress exhibited on a membrane structure of an external tank. This pre-cracked configuration could be thought of as an inherent material flaw, possible damage that occurred during launch, or an older component of a space asset that has pre-existing hypervelocity impact damage. A nylon 6-6 right cylindrical slug 1.8 mm in diameter and length, was shot at the target plate at velocities ranging from 3 to 7 km/s. All experiments were conducted under vacuum between 0.13 and 2.4 kPa (1–18 Torr). The material and optical properties used in the analysis for Mylar and Homalite 100 are listed in Table 1.

Dynamic optical techniques were configured in transmission and combined with high-speed photography which could capture eight frames down to the nanosecond scale of the complex stress wave patterns during impact; as well as subsequent dynamic fracture behavior of the impacted material. A thin film of Mylar (12.7 μm) was placed at a known distance ahead of the target plate and created a flash when the incoming projectile passed through it. This flash was registered by a visible wavelength photodiode and was used to trigger the ultra high-speed camera (Cordin 214, 100 million frames per second). At that same instant, a second high-speed camera (Photron SA-1, 1 million frames per second) with continuous recording capabilities of up to 1.2 s was triggered off the same photodiode, capturing a video of the incoming micrometeoroid, the impact event itself, and resulting energetic phenomena of plasma formation and ejecta (Fig. 2). The Photron was also used to discern the time of flight between the pre-target film and the polymer target plate, and then used to calculate the micrometeoroid velocity to an accuracy of ±2%.

Resulting crack velocities were estimated with a secant method which evaluates the derivative of the crack length versus time history provided by the output of the Cordin high-speed camera. It should be noted that, while cracks can locally accelerate and decelerate with virtually instantaneous accelerations, crack velocities in these tests were calculated only in the global sense dictated by the interframe time on the high-speed camera images. Thereby the estimated crack velocities were insensitive to any transient effects at the crack tip appearing on a smaller time scale.

Early efforts utilizing high-speed photography in dynamic fracture by Wells and Post in 1958 [8], and later Irwin et al. [9], Kobayashi [10] and Roskais [11], among others, coupled with optical diagnostics have developed experimental methods to determine the crack tip stress-state via the dynamic stress intensity factor. The two main optical diagnostics used in this study

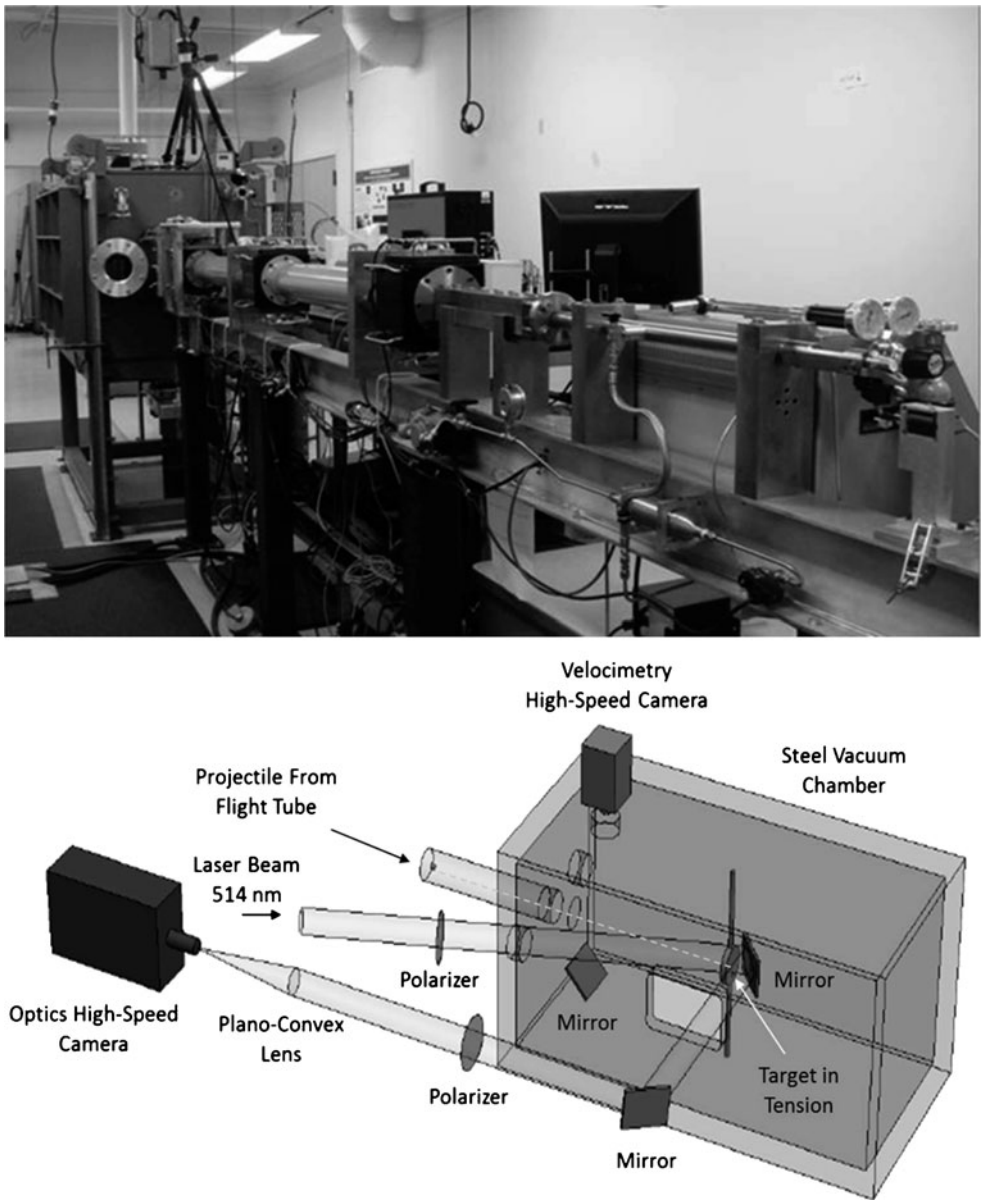

Fig. 1 (*Top*) SPHIR Two-stage light-gas gun facility developed for hypervelocity impact testing. (*Bottom*) Schematic of diagnostics used during testing including high-speed photography for velocimetry, and optical diagnostics for dynamic photoelasticity and caustic analysis of the target, to scale [7]

include dynamic photoelasticity and caustics. Each technique is mutually exclusive in that photoelasticity relies on the interference of light, and caustics on light refraction.

Dynamic Fracture Theory

By assuming the validity of the principles of singular fracture mechanics in a mode-I, or crack-opening

Table 1 Elastic and optical properties of Homalite 100 and Mylar

		Homalite 100	Mylar
Elastic modulus (MPa)	E	3,860	5,100
Poisson's ratio	ν	0.35	0.38
Density (kg/m^3)	ρ	1,230	1,390
P wave speed[a] (m/s)	c_l	2,145	2,447
S wave speed (m/s)	c_s	1,082	1,185
Rayleigh wave speed (m/s)	c_R	980	1,070
Stress optical coefficient (m^2/N)	c	-9.2×10^{-11}	-1.4×10^{-10}

[a]Determined by averaging 2 amplitudes from pulse-echo ultrasonic technique ±175 m/s

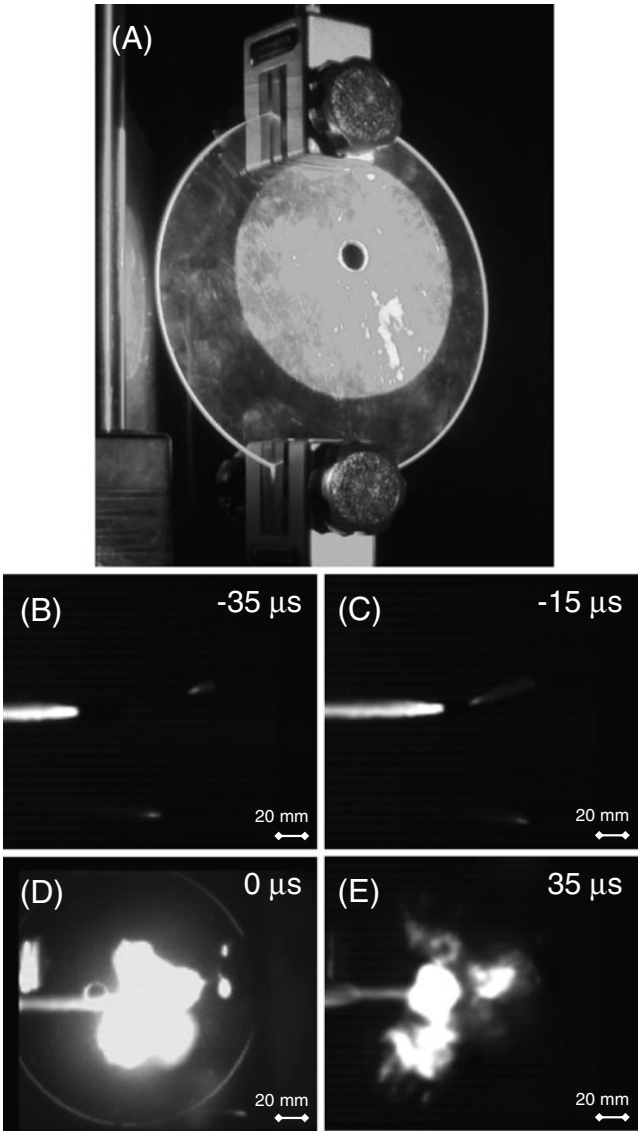

Fig. 2 (**a**) Photograph of 150 mm diameter, 1.6 mm thick polymer plate held in a load frame inside the two-stage light-gas gun with collimated laser beam illumination around a 20 mm hole. (**b**) High-speed photography (Photron SA-1, 200,000 frames per second, 128 × 112 resolution, 1 µs exposure time) captures a laboratory micrometeoroid or space debris, self-illuminated, as it flies through the field of view from *left* to *right*, creating a streak of ionized gas in its path 35 µs before impact. (**c**) At 15 µs before impact, the nylon slug is closer to the polymer plate and has an impact velocity of 5.2 km/s. (**d**) Spectral flash and plasma formation created on impact with the polymer plate. (**e**) Ejecta shown 35 µs after impact with considerable localized heating present

mode, the stresses at the vicinity of a crack propagating with velocity $v(t)$ can be described by the singular stress field as

$$\sigma_{ij} = K_I^d/\sqrt{2\pi r}\, f(\theta, v) \tag{1}$$

where in a polar coordinate system (r, θ) translating with the crack, r is equal to the radial distance from the crack tip and θ defines the angular position.

The common amplitude of all stress components is the dynamic stress intensity factor, $K_I^d(t)$, which varies explicitly with time as well as with the time-dependent crack tip speed, $v(t)$, and the applied loading, $P(t)$, and can be determined experimentally.

For growing cracks the dynamic stress intensity factor is

$$K_I^d(t, v(t), P(t)) \tag{2}$$

and should attain a critical value, denoted as K_{IC}^d and called the dynamic fracture toughness, which represents the material's resistance to dynamic crack growth. In the case of dynamically growing mode-I cracks, this resistance is crack growth rate dependent and has been found to be a function of the crack growth speed, v, which is argued by Rosakis et al. [12–14], among others, to be a material functional property and can be used in designing against catastrophic failure.

In the experimental configuration, designed such that the dynamic fracture toughness can be measured by optics, the polymer target plate is placed slightly out of the focus of the high-speed camera by a known distance, z_0. When laser light passes through the polymer specimen, there is a local thinning effect near the crack tip. In this region the light is consequently refracted away from the crack tip creating a characteristic shadow spot, surrounded by a brighter epicycloid called a caustic.

For mode-I dynamically propagating cracks in a presumed isotropic, homogeneous, linear elastic material, the crack tip velocity and dynamic stress intensity factor are both allowed to be arbitrary functions of time. If the plate is thin enough that the plane stress assumption is valid, it can be shown [15] that this optical retardation at the vicinity of the crack tip is directly proportional to the thickness average of the first stress invariant $\hat{\sigma}_{11} + \hat{\sigma}_{22}$ asymptotically expressed as

$$\hat{\sigma}_{11} + \hat{\sigma}_{22} = F(v)\frac{K_I^d(h)}{\sqrt{2\pi r_l}}\cos(\theta_l/2) + O(1) \text{ as } r_l \to 0 \tag{3}$$

where

$$F(v) = \frac{2(1+\alpha_s^2)(\alpha_l^2 - \alpha_s^2)}{[4\alpha_l\alpha_s - (1+\alpha_s^2)^2]} \tag{4}$$

$$\alpha_{l,s} = \sqrt{1 - \frac{v(t)^2}{c_{l,s}^2}} \tag{5}$$

$v(t)$ is the instantaneous crack speed, $c_{l,s}$ the material's pressure and shear wave speeds, respectively; and $K_I^d(t)$

is the instantaneous value of the dynamic stress intensity factor where

$$r_l = \sqrt{(x_1^2 + (\alpha_l x_2))^2};\ \theta_l = \tan^{-1}((\alpha_l x_2)/x_1)$$

so that the distorted polar coordinate system (r_l, θ_l) translates with the moving crack tip.

When utilizing caustics, the stress intensity factor, K_I, can be related to the experimentally measurable shadow spot diameter, D, by

$$K_I^d = \frac{2\sqrt{2\pi}}{3\alpha_l c h z_0 F(v)} \left(\frac{D(t)}{3.17}\right)^{5/2} \tag{6}$$

where c is an optical constant and h is the sample thickness, as shown by Rosakis [15], and Beinert and Kalthoff [16]. If the crack is growing with a certain speed, then by definition K_I^d equals its critical value (of dynamic fracture toughness, K_{IC}^d) for that speed and expression (equation (6)) directly furnishes the dynamic fracture toughness.

Moreover, the critical level of the energy that the surrounding material supplies to a dynamic, mode-I, crack tip growing at speed $v(t)$ is called the dynamic energy release rate, $G_{IC}^d(v)$, and can be related to the critical fracture resistance, K_{IC}^d, by

$$G_{IC}^d = \frac{1}{H} A_I(v) {K_{IC}^d}^2. \tag{7}$$

Here A_I is a universal function of crack speed, v, and the material's shear and pressure wave speeds, c_s and c_l, [17] and is expressed by

$$A_I = \frac{v^2 \alpha_l}{(1-\nu)\, c_s^2 B} \tag{8}$$

where

$$B = 4\alpha_l \alpha_s - \left(1 + \alpha_s^2\right)^2 \tag{9}$$

and the term H is a combination of the Young's Modulus, E, and the Poisson's ratio, ν, and is given by

$H = E$ for plane stress and

$H = E/(1-\nu^2)$ for plane strain.

By using caustics, we presupposed that the fracture process is mode-I or crack opening dominant and that small scale yielding in the area of the crack tip does not effect the caustic; therefore assuming the crack can be adequately described by the asymptotic stress solution [18]. Then based on the experimental results, we determined if that fracture criterion assumption was valid under these complex conditions. The relation (equation (7)) demonstrates that if indeed the dynamic fracture toughness, K_{IC}^d, is a material dependent function of crack speed, v, so is the critical level of required energy, G_{IC}^d. Consequently, G_{IC}^d is also considered to be a function characterizing the material's ability to resist fracture and can be thought of as the requisite energy dissipated at the crack tip during the dynamic fracture process [17]. One of the major goals of the study is to directly measure this function in the presence of highly energetic hypervelocity impact loading conditions.

Uncertainty in Data Analysis

While this investigation is limited to brittle materials, errors in the calculation of the dynamic stress intensity factor come from possible crack tip transient and three-dimensionality (3-D) effects, potential material optical anisotropy, and the time mismatch of the high-speed camera interframe time with the rapidly changing

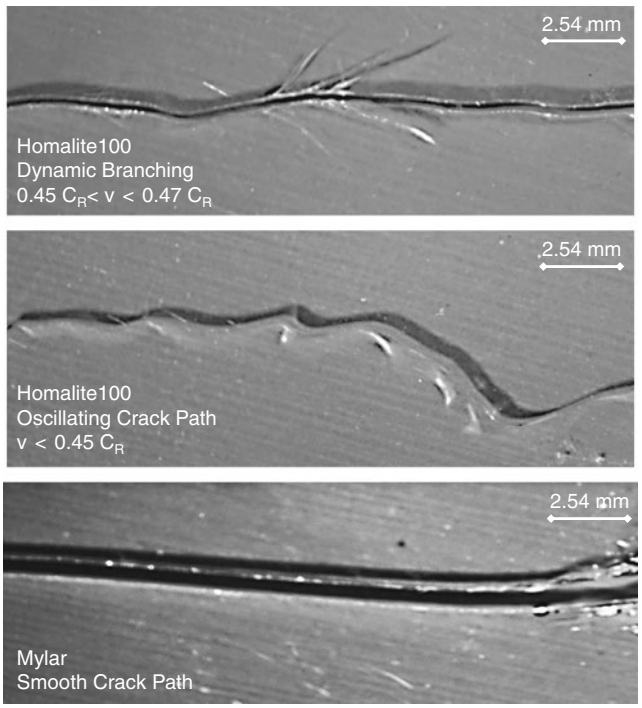

Fig. 3 (*Top*) Homalite 100 resulting crack path appearance in the rare case where crack speed exceeded 0.45 c_R, the Rayleigh wave speed, and the crack path would branch. Average branching angle was approximately 29°. (*Middle*) Homalite 100 typically resulted in a crack path exhibiting distinctive kinking or oscillations. (*Bottom*) Mylar exhibited a smooth crack path appearance

behavior at the crack tip; all of which could affect the interpretation of the caustic.

The benefit of utilizing the optical method of caustics is that the measurement is made directly at the crack tip, and consequently the interpretation of the data does not rely on the complete transient stress analysis of the entire specimen [15]. By using this method, the domain around the crack is assumed to exhibit typical square root stress singularity at all times. Due to the 3-D effects at the crack tip, an innate limitation on time resolution, shown to be on the order of at least $h/2c_s$ or sample thickness over twice the shear wave speed, exists [19]. For our study it would be on the order of less than 1 μs. Moreover it has been shown that the K–v relation is not necessarily a unique representation, suggesting that the stress intensity factor may change with time without any change in crack tip velocity. This leads to scatter within the general trend of increasing stress intensity factor with increasing crack velocity [19], particularly at the higher crack velocities as seen in Figs. 5 and 6.

To mitigate error in the interpretation of the caustic and crack tip velocity, only data from tests where the cracks did not exhibit arrest have been used in the

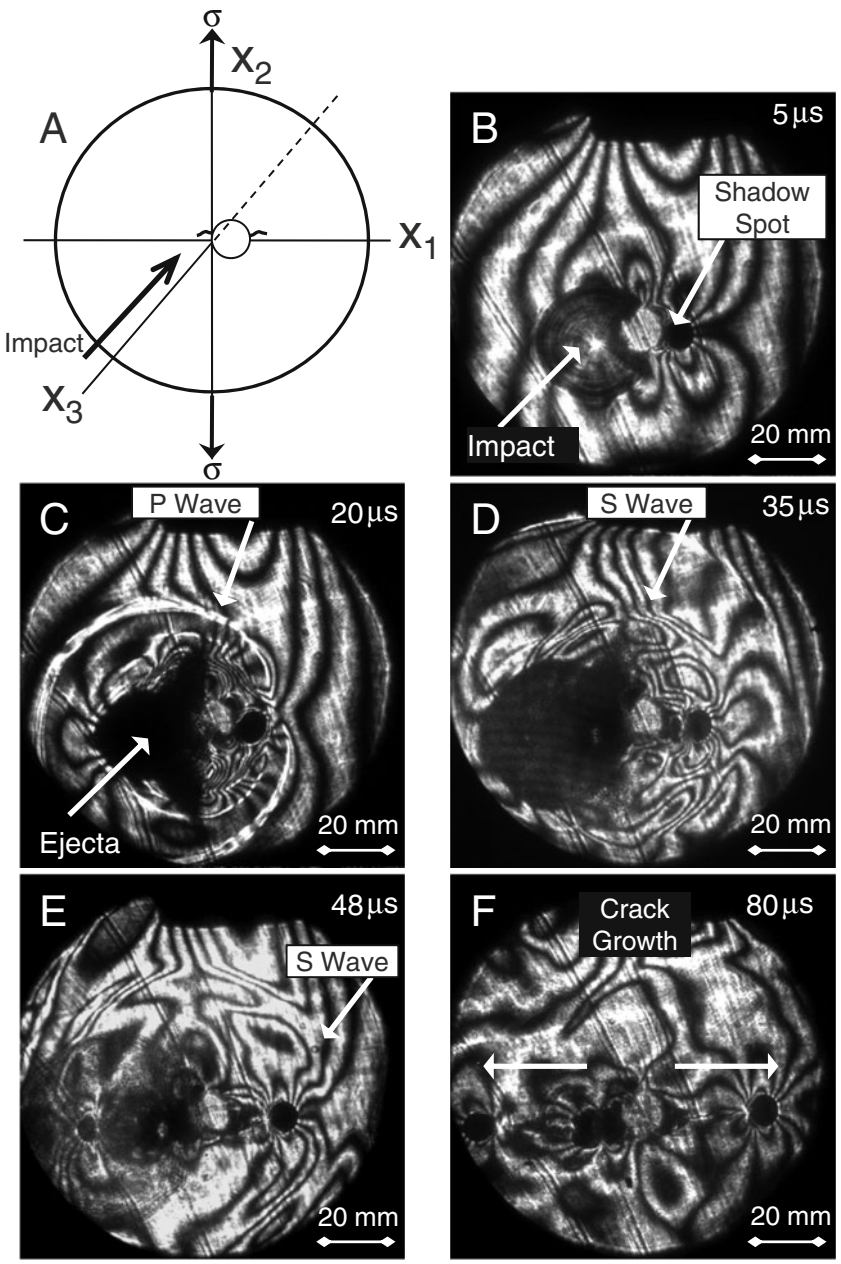

Fig. 4 High-speed photography (Cordin, full resolution, 50 ns exposure time) is used to capture the isochromatic fringe pattern, caustics and shadow spots generated during crack growth resulting from a micrometeoroid or space debris hypervelocity impact on Mylar. (**a**) Configuration of the pre-cracked polymer plate, in plane x_1 and x_2 prior to hypervelocity impact loading from the x_3, out-of-plane, direction. (**b**) Upon impact, the shadow spot shown has not yet felt the impact shock. (**c**) The fastest stress wave, the longitudinal wave, travels radially outward from the impact site at 2447 km/s and disturbs the caustic, but there is no crack growth. Ejecta is thrown from the plate and clouds the field of view. (**d**) The crack begins to grow, ejecta is starting to disperse and the shear wave is seen moving radially outwards from the impact site at 1,185 m/s. (**e**) The crack appears to grow just behind the shear wave. (**f**) After 80 μs the polymer plate has almost completely failed, cracks speeds averaged 360 m/s (800 mph)

analysis. The reason for this is to avoid sudden transients in the form of either crack tip speed, acceleration, or deceleration. As shown by Rosakis and coworkers [20–22], transients are known to effect the ability of caustics to accurately measure the dynamic value of transient stress factors. The work of Tippur et al. [23] also elucidates the effect of transients in relation to the optical method of coherent gradient sensing (CGS).

Additionally, optical distortions resulting from the large beam expansion (100 mm) have been removed using MATLAB, specifically employing the Control Point Selection Tool in the Image Processing Toolbox. Before each test, a high-speed camera image is taken with a calibrated grid placed in the field of view. The experimental grid image is then mapped using a bi-cubic transformation to a virtual grid of the exact measured size in MATLAB. After a hypervelocity test is run, the resulting caustic images with the same field of view are post-processed through the code to map the test images to the virtual grid, consequently removing chromatic error. From there the caustic diameter and crack tip position is measured using ImageJ (image processing

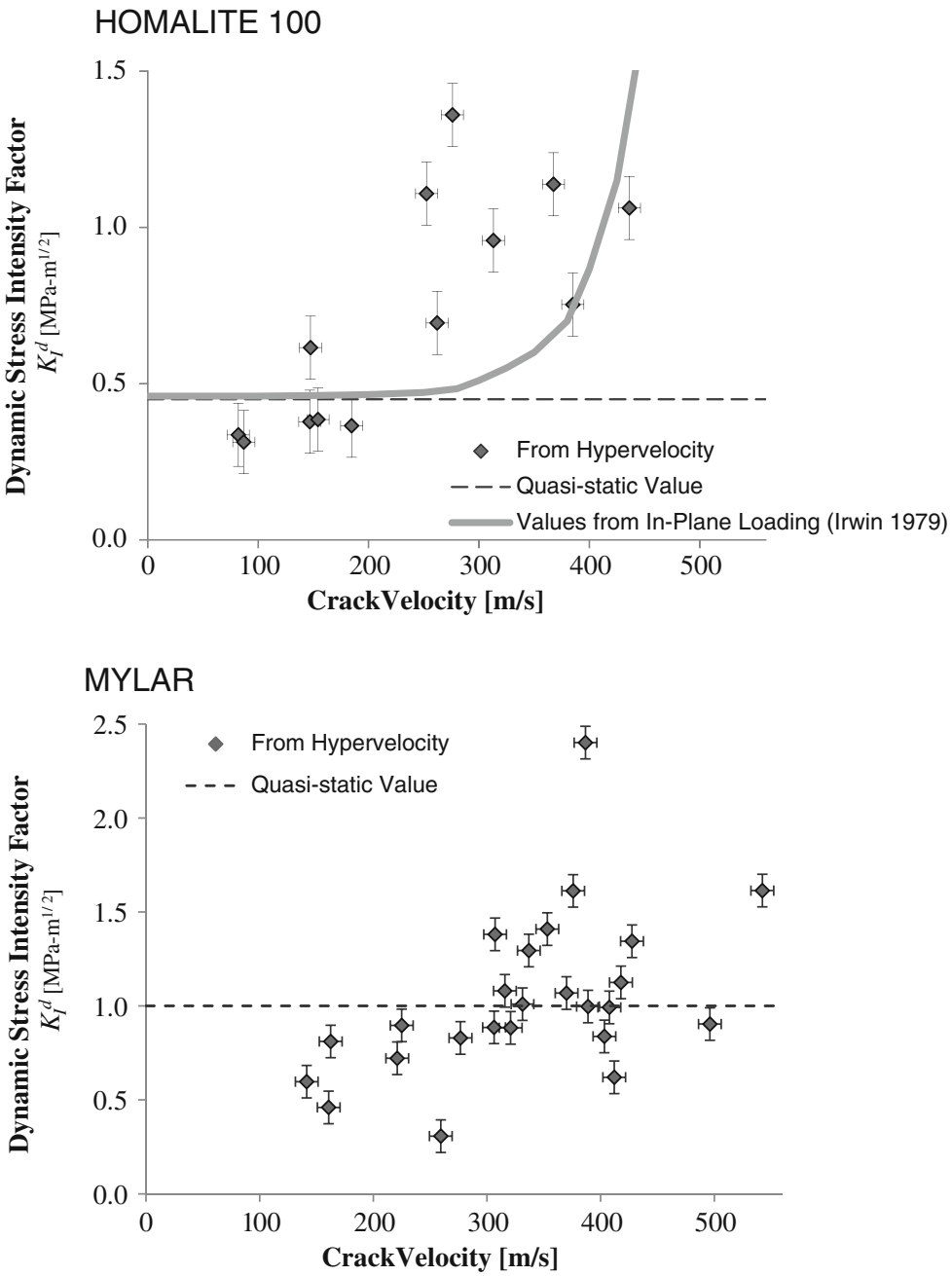

Fig. 5 Dynamic stress intensity factor at the crack tip as a function of crack speeds resulting from hypervelocity impact induced fracture on Homalite 100 (*top*) and Mylar (*bottom*) thin plates. The quasi-static stress intensity value is labeled by a dashed line across the horizontal axis. Homalite 100 data points are averaged per test. Mylar data points are not averaged per test since the mode-I fracture trend was clear before averaging. For Homalite 100, the hypervelocity results are compared to the characteristic gamma-shaped K–v curve exhibited by conventional mode-I in-plane loading tests at a much lower rate on single edge notch (SEN) specimens by Irwin [9]

program), and is an average of three readings of the measurement, having first calibrated the length scale using the grid image. In this regard, uncertainty in the position of the crack tip, measured at a distance r at any instant captured is less than 10 mm or 7% of the field of view, and uncertainty in the shadow spot diameter or D, is on the order of less than 1%.

Results

Both polymers had crack velocities sustain global subsonic speeds of roughly 0.2–0.47 c_R, the Rayleigh wave speed, but Mylar tended to have slightly higher crack velocities. We believe this is due to the degree of transient effects at the crack tip which appears to have a material dependence. Homalite 100 upon impact exhibited a distinctive kinking in the crack path appearance, and took slightly longer (20 μs on average) than Mylar to reach complete failure of the plate. Conversely, Mylar exhibited a flat crack path appearance that closely followed the shear wave, and grew perpendicular to the direction of the far-field tensile loads. This may be due to the fact that impact longitudinal and shear waves on the Homalite 100 target had more time to reflect from the boundaries and interact with each other (Fig. 3). Consequently, complex wave interaction of Homalite 100 influenced transient crack behavior, and as a result the crack appears to be following instantaneous local mode-I, or local opening crack path.

No statistically significant correlation was found between location of the impact and time of crack transition to propagation, nor between the pre-tensile far-field load level and the crack transition to propagation, respectively. The former observation is possibly due to the inherent variability in the pre-cracks along with the difficulty to visualize the stress state at the crack tip immediately upon impact from ejecta clouding the view, and the latter most likely due to the fact that the inertia of the incoming projectile exceeds the existing stress from the pre-tensile load as well as the material strength of the thin plate. It should be noted that from the high energy generated during hypervelocity impact, intense localized heating occurs caused by the isentropic mismatch of initial shocking and rarefaction wave interaction between the plate and the impactor. This process causes the projectile to vaporize on impact, as would happen to space debris in low earth orbit and micrometeoroids in outer space.

Overall, Mylar exhibited less transient behavior and an unadulterated isochromatic fringe pattern from photoelasticity than Homalite 100 due to the fracture process taking less time with less influence from impact wave interaction and boundary reflection, as shown in Fig. 4. Regardless, all cases exhibited a fracture criterion of mode-I in an averaged sense and a stress field that was driven by the longitudinal waves dictating plate fracture behavior (Fig. 5). Table 2 summarizes the results of the investigation.

Table 2 Results from optical investigations of hypervelocity impact dynamic fracture of brittle polymers

	Homalite 100	Mylar
Average crack tip speed (m/s)	230	330
Quasi-static fracture toughness[a] (MPa-$\sqrt{\text{m}}$)	0.45	1.1
Averaged dynamic stress intensity (MPa-$\sqrt{\text{m}}$)	0.73	1.1
Quasi-static energy release rate (J/m^2)	52.5	196
Averaged dynamic energy release rate (J/m^2)	208	284
Crack path appearance	Oscillating	Flat

[a]From literature, Mylar from Shockey [24], Homalite 100 from Mall and Kobayashi [14]

Conclusions

The continuum approach underlying elastodynamic fracture theory often breakdowns under high loading and, or strain rates since it dictates that crack behavior must consume energy at the rate is it delivered to it by the surrounding continuum via altering speed. However laboratory micometeoroid and orbital debris stikes on brittle polymers averaging 6 km/s and producing strain rates as high as 10^{-11} s^{-1} have shown otherwise. The results of this investigation illustrate that the mode-I asymptotic stress solution at the crack tip remains a valid approach in characterizing fracture behavior resulting from micrometeoroid and space debris hypervelocity impacts with extreme conditions of mixed-mode loading, highly localized heating, and complex impact phenomena of ejecta and plasma formation. A reason for this behavior is that the speed of the incoming micrometeoroid is on the order of two to three times faster than the material longitudinal and shear wave speeds. As such the slowest waves, Rayleigh surface waves, do not have enough time to propagate and interact with boundaries. Consequently no significant out-of-plane bending mode is generated before the plate has completely failed. We have discovered that laboratory micrometeoroids and orbit debris impacts of Mylar and Homalite 100 do exhibit, in an averaged sense, mode-I dominance. As a result, this criterion can be introduced in models to predict damage

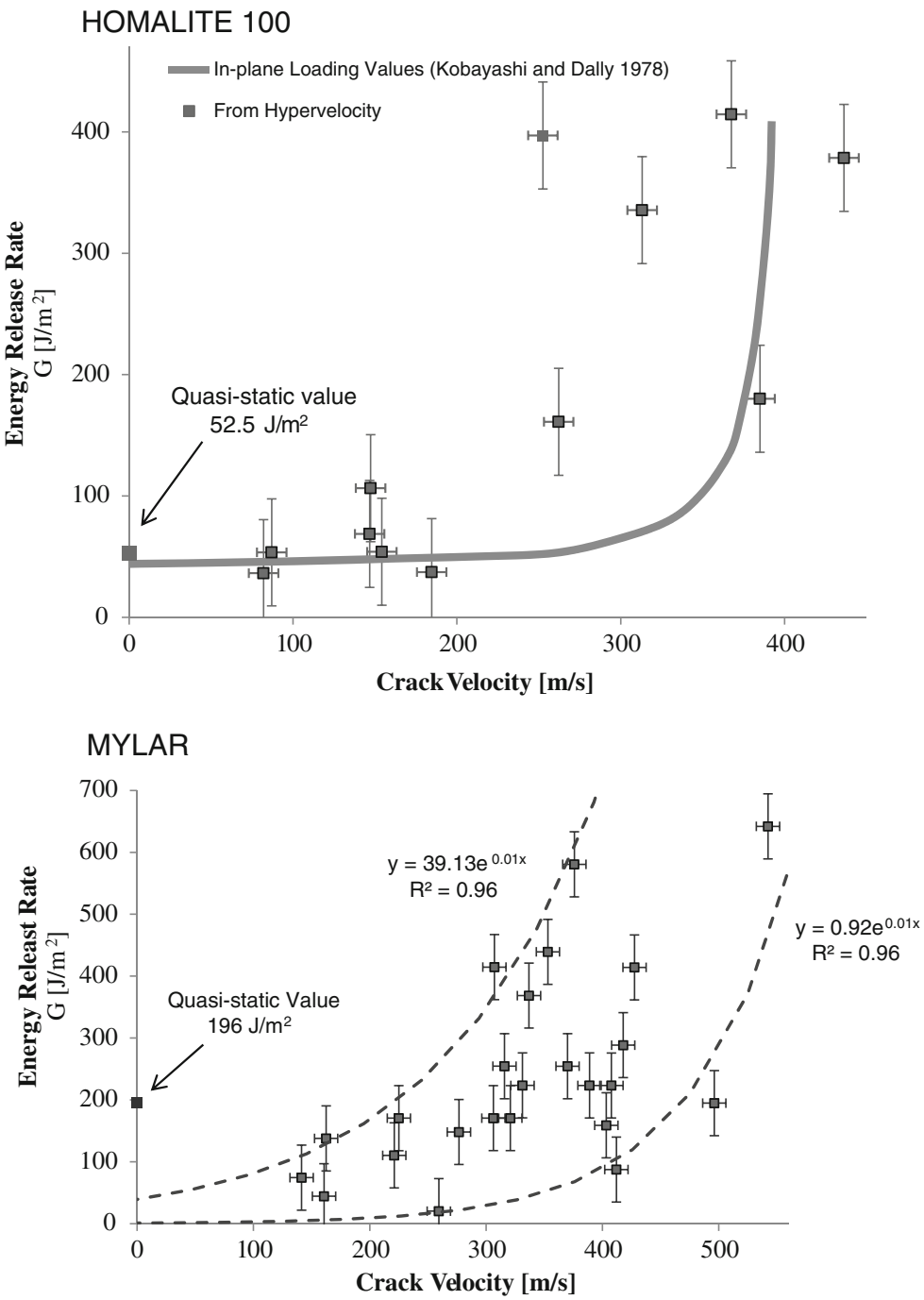

Fig. 6 Averaged dynamic energy release rates at the crack tip as a function of crack speeds resulting from hypervelocity impact induced fracture on Homalite 100 (*top*) and Mylar (*bottom*) thin plates. The quasi-static energy release rate value ($v = 0^+$) is labeled on the vertical axis. For Homalite 100, the *solid line* illustrates averaged values from numerous geometries tested in conventional, purely mode-I or crack-opening configurations, with in-plane loading conditions at much lower rates [16, 25]. For Mylar, the four largest and four smallest values of the energy release rate per 100 m/s of crack velocity are used to generate upper and lower exponential curve fits, illustrating the envelope of the overall trend of increasing energy release rate with increasing crack velocity seen in the hypervelocity data

under these extreme conditions. Overall, longitudinal waves from the initial impact dictate stress at the crack tip, and failure of the plate is dominated by in-plane loading.

A couple of significant observations can be made on the basis of the results displayed in Figs. 5 and 6. In both material systems tested, the critical energy provided to the crack tip for growth appears to have a well-defined dependence on crack tip speed. This dependence exhibits a drastic increase in G^d_{IC} at about 0.4 c_R. For Homalite 100, this value is close to the crack branching speed [10]. Perhaps the most significant observation is that the characteristic gamma shape G–v curve shown in the line obtained from averaging multiple in-plane loading configurations at much lower structural loading rates lies within the current experimental results that have been obtained under loading conditions involving extremely energetic out-of-plane hypervelocity impacts

[10, 16, 25]. The consequence of these observations is that classical mode-I dynamic fracture mechanics criteria still remain valid during hypervelocity impact and as a result, dynamic fracture methodologies can still be used for the safe design of thin shell space structures.

The above conclusion can be rationalized by emphasizing that in the specific hypervelocity impact investigations examined, the projectile (a.k.a. micrometeoroid or space debris) completely inserts itself in the thin polymer target with speeds that are up to seven times greater than the Rayleigh surface wave speeds of the target. As a result, the insertion process is completed on a time period which is of the order of a third of a microsecond and involves almost instantaneous release of extreme amounts of surface energy, similar to an embedded localized explosion. Due to the small thickness of the target, and the extremely fast insertion process, much of this energy is available for in-plane stress generation and in-plane crack driving force creation. Moreover, the entire crack growth process following projectile insertion takes place well before multiple reflected waves from the boundaries have the time to fully develop an out-of-plane flexural (bending) mode of plate deformation.

Acknowledgements Research support including the Caltech Center for Predictive Science Academic Alliance Program (PSAAP) with funding from the Department of Energy (DOE) Award Number DE-FC52-08NA28613 through the National Nuclear Security Administration (NNSA), the National Science Foundation (NSF), and the National Aeronautics and Space Administration (NASA) through the American Society of Engineering Education (ASEE) is gratefully acknowledged.

References

1. N.R. Council (1997) Protecting the space station from meteoroids and orbital debris. National Academy Press, Committee on International Space Station Meteoroid/Debris Risk Management, Aeronautics and Space Engineering Board
2. Portree D, Loftus J Jr (1999) Orbital debris: a chronology. Tech. Rep. TP-1999-208856, NASA
3. Hill S (2004) Determination of an empirical model for the prediction of penetration hole diameter in thin plates for hypervelocity impact. Int J Impact Eng 30:303
4. Cunn M (2010) International space station gets a bay window. sci-tech-today.com
5. Stockman HS (2006) James Webb Space Telescope. In: Proceedings of the International Astronomical Union, pp 522–523
6. Grosch D, Riegel J (1992) Development and optimization of a "Micro" two-stage light-gas gun. In: Hypervelocity impact proceedings symposium
7. Figueroa F (2010) SolidWorks image. Created in Professor Veronica Eliasson's research group at the University of Southern California
8. Wells A, Post D (1958) The dynamic stress distribution surrounding a running crack. In: Proceedings for the Society of Experimental Stress Analysis, vol 16, pp 69–96
9. Irwin G, Dally J, Kobayashi T, Fourney W, Etheridge M, Rossmanith H (1979) On the determination of the a-K relationship for birefringent polymers. Exp Mech 19:121
10. Koybayashi A, Mall S (1978) Dynamic fracture toughness of Homalite-100. Exp Mech 18:11
11. Rosakis A (1980) Analysis of the optical method of caustics for dynamic crack propagation. Eng Fracture Mech 13:331
12. Rosakis A, Zehnder A (1985) On the dynamic fracture of structural metals. Int J Fracture 27:169
13. Kobayashi A, Dally J (1979) Dynamic photoelastic determination of the a-K relation in 4344 alloy steel. In: Crack arrest methodology and applications
14. Kobayashi A, Emery A, Mall S (1976) Dynamic finite element and dynamic photoelastic analyses of two fracturing Homalite-100 plates. Exp Mech 16:321
15. Rosakis A (1993) Two optical techniques sensitive to gradients of optical path difference: the method of caustics and the coherent gradient sensor (CGS), Chapter 10. Experimental techniques in fracture. Wiley, New York
16. Beinert J, Kalthoff J (1981) Experimental determination of dynamic stress intensity factors by shadow patterns. In: Experimental evaluation of stress concentration and intensity factors. Martinus Nijhoff
17. Freund L (1990) Dynamic fracture mechanics. Cambridge University Press, Cambridge
18. Freund L, Clifton R (1974) On the uniqueness of plane elastodynamics solutions for running cracks. J Elasticity 4:293
19. Knauss W, Ravi-Chandar K (1986) Fundamental considerations in dynamic fracture. Eng Fracture Mech 23:9
20. Krishnaswamy S, Rosakis A (1991) On the extent of dominance of asymptotic elastodynamic crack-tip fields; part I: an experimental study using bifocal caustics. J Appl Mech 58:87
21. Freund L, Rosakis A (1992) The structure of the near-tip field during transient elastodynamic crack growth. J Mech Phys Solids 40:699
22. Liu C, Rosakis A, Freund L (1993) The interpretation of optical caustics in the presence of dynamic non-uniform crack-tip motion histories: a study based on a higher order transient crack-tip expansion. Int J Solids Struct 30:875
23. Tippur H, Rosakis A (1991) Quasi-static and dynamic crack growth along bimaterial interfaces: a note on crack-tip field measurements using coherent gradient sensing. J Exp Mech 31:243
24. Shockey D (1981) Fracture of structural materials under dynamic loading. Tech. Rep. AFOSR-TR-0402, Air Force Office of Scientific Research
25. Kobayashi T, Dally J, Fourney W (1978) Influence of specimen geometry on crack propagation and arrest behavior. In: VIth international conference of experimental stress analysis, pp 18–22